Neutron-scattering study of incommensurate magnetic order in the heavy-fermion superconductor UNi_2Al_3

J. G. Lussier, M. Mao,* A. Schröder,† J. D. Garrett, and B. D. Gaulin
Department of Physics and Astronomy, McMaster University, Hamilton, Ontario, Canada L8S 4M1

S. M. Shapiro
Department of Physics, Brookhaven National Laboratory, Upton, New York 11973

W. J. L. Buyers
National Research Council, Neutron Program for Materials Research, Chalk River Laboratories, Chalk River, Ontario, Canada K0J 1J0
(Received 9 April 1997; revised manuscript received 17 June 1997)

Elastic neutron scattering from a single-crystal sample of the heavy-fermion superconductor UNi_2Al_3 has revealed the onset of long-range magnetic order below $T_N=4.6$ K. This order is characterized by an incommensurate (IC) ordering wave vector given by $(\frac{1}{2}\pm\tau, 0, \frac{1}{2})$ with $\tau=0.11\pm0.003$. The intensity of several magnetic satellite Bragg peaks within the $(h,0,l)$ plane is well described by a model in which the spins lie within the basal plane and are modulated in amplitude from site to site. By applying a magnetic field to select from all the possible domains, we find that the moment is polarized along the **a** direction, with a maximum amplitude of $0.21\pm0.1\mu_B$ per uranium atom. The order-parameter exponent β associated with this transition is $0.34\pm.03$, which is typical of three-dimensional ordering transitions. Measurements down to $\sim$0.3 K show that the magnetic order coexists with superconductivity below $T_C\sim1.2$ K, and that these states are coupled as shown by anomalous behavior of the magnetic order parameter around T_C. Measurements were also made in magnetic fields of up to 8 T applied perpendicular to the $(h,0,l)$ plane, along $(-1,1,0)$, a near-neighbor direction within the hexagonal basal plane. While the field does not influence T_N, it does increase the intensity of the magnetic Bragg peaks by a factor of $\sim$1.5, as well as increase the IC part of the ordering wave vector at low temperatures. [S0163-1829(97)01441-0]

INTRODUCTION

Heavy-fermion materials have been at the forefront of condensed matter research due to the exotic behavior displayed by their thermodynamic and transport properties at moderate temperatures, as well as the usual coexisting ground states which a subset of these metals display at low temperatures.[1] At high temperatures they are usually poor metals, the temperature dependence of whose resistivity is often characteristic of semiconductors. They can be characterized by up to three temperature scales. A relatively high-temperature coherence temperature is usually present, below which the resistivity decreases on cooling, while at low temperatures some of these materials enter one or more ordered phases. Most of the interest in these materials has focused on the few compounds which display microscopic coexistence of antiferromagnetism and superconductivity at low temperatures. Within the conventional BCS theory of superconductivity, electrons of opposite momentum at the Fermi surface and of opposite spin form composite Cooper pairs which participate in the supercurrent. Magnetism is usually thought of as being incompatible with this scenario as it can provide spin-flip electron scattering which breaks up the Cooper pairs.

There are four known uranium-based heavy-fermion metals which exhibit the apparent microscopic coexistence of antiferromagnetism and superconductivity at low temperatures. UPt_3 (Ref. 2) forms a hexagonal-closed-packed structure and orders antiferromagnetically below $\sim$6 K. It then undergoes two superconducting transitions near $T_C\sim0.5$ K.[3] The multiple nature of the superconducting transition is believed to result from symmetry breaking within the hexagonal basal plane due to the magnetic long-range order displayed by UPt_3. Pressure causes the two superconducting transitions to merge, and the ordered magnetic moment decreases to zero, so as to produce a tetracritical point in its pressure-temperature phase diagram.[4] Body-centered-tetragonal URu_2Si_2 (Ref. 5) undergoes antiferromagnetic and superconducting phase transitions at 17 and $\sim$1.2 K, respectively. The long-range magnetic order displayed by both these materials is highly unusual in that it is characterized by extremely small ordered moments $\mu_{ord}\sim0.02\mu_B$ for UPt_3 (Ref. 2) and $\mu_{ord}\sim0.04\mu_B$ for URu_2Si_2.[6,7] Although these anomalously small ordered moments have led to speculation[8] that the order which they display is nontrivial and involves multispin rather than dipole ordering, this has *not* been borne out by recent measurements.[9]

Recently, two additional heavy-fermion metals have been discovered in which superconductivity and antiferromagnetic order also coexist. These are the simple hexagonal intermetallics UPd_2Al_3 (Ref. 10) and UNi_2Al_3 (Ref. 11) which respectively undergo transitions to antiferromagnetism at $T_N\sim14.5$ and $\sim$4.6 K, and to superconductivity at $T_C\sim2$ and 1.2 K. Extensive neutron-scattering measurements[12,13] on UPd_2Al_3 show that it orders in a simple $\mathbf{Q}=(0,0,\frac{1}{2})$ antiferromagnetic structure in which the moments lie in the basal

plane, in ferromagnetic sheets that are antiparallel to those in adjacent basal planes. There is also good evidence for a phase transition involving a moment direction reorientation within the basal plane at temperatures near but below T_N.[14] However, all measurements are consistent with a sizable ordered moment $\mu_{\rm ord} \sim 0.85\mu_B$.

For UNi_2Al_3, we report elastic neutron-scattering measurements on a single crystal which show that it undergoes a transition at $T_N \sim 4.6$ K to a state with long-range, incommensurate magnetic order characterized by the wave vector $\mathbf{Q}=(\frac{1}{2}\pm\tau,0,\frac{1}{2})$ with $\tau=0.11\pm0.003$. Preliminary accounts of this work have appeared elsewhere.[15] This magnetic order is associated with moments at the uranium site. There is no evidence for any magnetism associated with the nickel site. In earlier neutron-diffraction measurements performed on powder samples of UNi_2Al_3 no evidence of magnetic order was obtained and an upper limit of $0.2\mu_B$ (Ref. 12) was placed on the size of any possible ordered moment. Muon spin rotation (μSR) experiments[16] on polycrystalline UNi_2Al_3 showed evidence for antiferromagnetism with an ordered moment of the order of $0.1\mu_B$. Uemura *et al.*,[17] in subsequent μSR work, noted that the μSR signal from UNi_2Al_3 was similar to that from the organic spin density wave system $(TMTSF)_2PF_6$, and suggested the possibility that the magnetic order in UNi_2Al_3 might be incommensurate. These measurements were performed on a crystal cut from the same boule as the crystal we have studied.

EXPERIMENTAL DETAILS

In comparison with the rather extensive literature which currently exists for its sister compound UPd_2Al_3, there is little information available on UNi_2Al_3, for which single crystals are harder to grow. Our crystal of UNi_2Al_3 was grown at McMaster University using the Czochralski tri-arc technique. No initial seeds were used (except for the tungsten tip). The starting materials were stoichiometric amounts of each of the elements in high purity form. The Al used was 99.9999% pure, the Ni was 99.999% pure, while the depleted U was from the same high-purity source from which other U-based heavy-fermion superconductors were grown.[7] Such high-purity starting materials are necessary because the magnetic and particularly the superconducting properties of this class of materials are sensitive to impurities.

The final cylindrical crystal, roughly 1 cm^3 in volume, was subsequently wrapped in tantalum and annealed in an evacuated quartz cell at 900 °C for one week. Small pieces cut from the boule were used to characterize the crystal. Uniform susceptibility measurements showed results consistent with earlier measurements,[11] a hump in the susceptibility near 80 K, with pronounced anomalies near $T_N=4.6$ K as well as a Meissner signal at $T_C \sim 1.2$ K. A neutron-diffraction pattern was taken of one such piece after it had been crushed to form a powder. Measurements made at 10 K (above T_N) and 3 K (below T_N) were consistent with single phase material to at least the 5% level. The large nuclear incoherent background from the Ni made it difficult to be more precise than this. In addition, the measurement gave no indication of any temperature-dependent scattering over this temperature range, consistent with earlier estimates[12] that the size of the ordered moment associated with this phase transition was less than $0.2\mu_B$/U site *on average*. We will see that our single-crystal measurements bear this out.

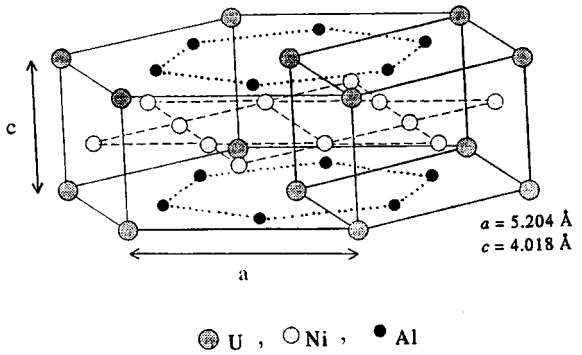

FIG. 1. The simple hexagonal crystal structure exhibited by UNi_2Al_3 is shown.

Neutron measurements on the single crystal revealed that it was comprised of three closely aligned grains, having a total mosaic spread of 2°. The crystal structure, shown in Fig. 1, belongs to the $P6/mmm$ hexagonal space group, in which the U atoms lie on a simple hexagonal lattice. The lattice constants at 4.2 K were $a=5.204$ Å and $c=4.018$ Å. The relative measured integrated intensities of six nuclear Bragg peaks (chosen to be weak ones to avoid problems with extinction) were found to agree very well with the intensities calculated for the structure shown in Fig. 1.

Elastic neutron-scattering measurements were carried out on this high-quality single crystal at the NRU reactor of the AECL's Chalk River Laboratories (CRL) as well as at the HFBR at Brookhaven National Laboratory (BNL). Three different spectrometer configurations were employed with the sample mounted in four different cryostats, two of which were equipped with vertical field, split coil magnets. The different cryostats were required to access both temperatures below the superconducting T_C, and relatively high temperatures above the ''hump'' in the uniform susceptibility at ~80 K.[11]

ZERO-FIELD MEASUREMENTS

Measurements were carried out at the E3 triple axis spectrometer at CRL with a Si(1,1,1) monochromator and a pyrolitic graphite, PG(0,0,2), analyzer set for zero energy transfer. Data were collected at neutron energies of 14.7 and 34.1 meV with a PG filter in the scattered beam to remove higher order contamination, as well as at 17.05 meV, without the filter. The (h,h,l), $(h,0,l)$, and $(h,k,0)$ high-symmetry planes were investigated by means of two-dimensional grid scans as well as with finer line scans along special directions. The scans were made at a temperature of 1.8 K, well below $T_N=4.6$ K, and also at a temperature of 20 K, well above T_N, in order to search for temperature-dependent scattering signifying magnetic order. Figure 2 shows the results of two such scans along the $(h,0,\frac{1}{2})$ direction, which clearly show a Bragg peak feature at both $(0.39,0,\frac{1}{2})$ and $(0.61,0,\frac{1}{2})$.

A survey of the $(h,0,l)$ scattering plane revealed the appearance of Bragg peaks of the form $(n/2\pm\tau,0,n/2)$ with n odd and $\tau=0.110\pm0.003$ at temperatures below ~5 K. As

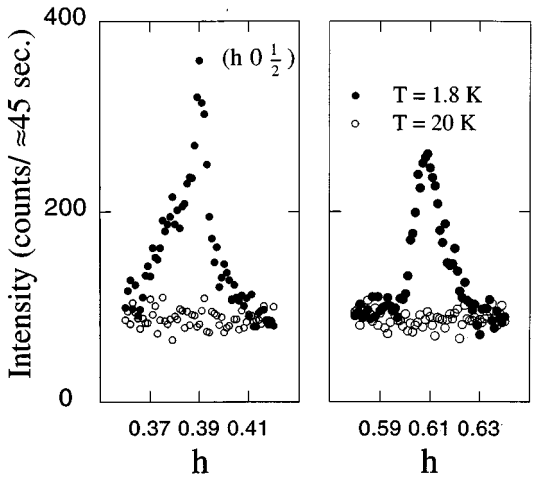

FIG. 2. Sections of a scan along $(h,0,\frac{1}{2})$ are shown at temperatures of 20 K (well above $T_N \sim 4.6$ K) and 1.8 K (well below T_N). These scans identify the incommensurate magnetic ordering wave vector as $(\frac{1}{2}\pm\tau,0,\frac{1}{2})$ with $\tau=0.110\pm0.003$. The asymmetric line shape is due to the sample mosaic.

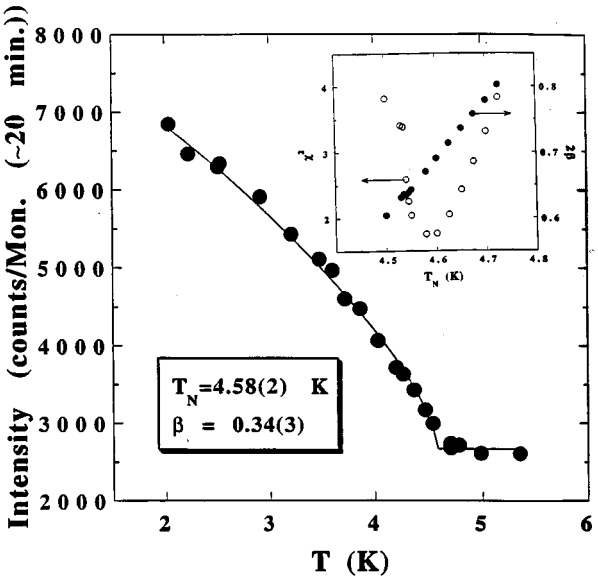

FIG. 3. Magnetic order parameter as measured at the $(0.61,0,\frac{1}{2})$ position is shown. The solid line corresponds to the best fit of the data to intensity $\sim[(T_N-T)/T_N]^{2\beta}$, with $T_N=4.58\pm0.02$ K and $\beta=0.34\pm0.03$. The inset shows the dependence of both β and the corresponding goodness-of-fit parameter χ^2 on T_N.

will be described, the temperature, field, and wave vector dependence of these superlattice Bragg peaks identify them as being magnetic in origin. No other temperature-dependent scattering was found during the course of the investigation of the three scattering planes. The component of the magnetic ordering wave vector within the hexagonal basal plane is incommensurate, $q_{\rm IC}=\frac{1}{2}\pm\tau$. It can be approximated as $q_{\rm IC}=\frac{1}{2}\pm\frac{1}{9}$, but there is no simple relationship between this magnetic ordering wave vector and any wave vector characterizing the chemical lattice. Because $l=n/2$, with n odd for the $(n/2\pm\tau,0,n/2)$ ordering wave vector, the magnetic structure along the c direction corresponds to a simple antiferromagnetic stacking of the basal plane structure, as also occurs in UPd_2Al_3.[12]

The intensity of the scattering at the magnetic Bragg peak positions is very weak. It is reduced by three orders of magnitude compared with a typical Bragg peak of nuclear origin, such as (1,0,0). The width of the magnetic Bragg peaks is found to be that determined by the resolution of the instrument, indicating true long-range magnetic order below T_N with a correlation length exceeding 400 Å. This contrasts with results reported in the appropriate antiferromagnetic phase of both UPt_3 (Ref. 2) and URu_2Si_2.[6,7] The asymmetric line shape of some of the magnetic Bragg peaks is due to the mosaic of our crystal.

Longitudinal scans of several magnetic Bragg peak positions were carried out as a function of temperature between ~2 and 10 K. These scans showed Gaussian line shapes with temperature-independent positions and peak widths, until the superlattice scattering disappeared near 5 K. Measurements with high-temperature stability were carried out at BNL on the H8 spectrometer with PG(0,0,2) as both monochromator and analyzer, a PG filter in the scattered beam, and the neutron energy set at 14.7 MeV. The peak intensity data shown in Fig. 3 was collected with the temperature stable to at least ±0.002 K, so as to allow a precise determination of both T_N and β, the critical exponent characterizing the rise of the staggered magnetization from zero at T_N. From fits to the data as a function of T_N shown in the inset to Fig. 3, we find that the best goodness-of-fit parameter χ^2 occurs for $T_N=4.6\pm0.05$ K, and $\beta=0.34\pm0.03$. The value for β is consistent with expectations for the three-dimensional Ising, XY, and Heisenberg universality classes.[18] The critical behavior is strikingly different from that observed in UPt_3 (Ref. 2) and URu_2Si_2,[6,7] for which the peak intensities grow linearly over an anomalously broad temperature range, consistent with a mean field, $\beta=\frac{1}{2}$ onset. However, it is similar to the critical behavior seen in UPd_2Al_3.[13] No hysteresis is observed in the order-parameter scan on heating and cooling, which suggests a continuous transition, despite the fact that there is no obvious critical scattering present above T_N. It is likely that the intensity of such critical scattering was simply too weak to be observed. The absence of the critical scattering means that β can be rather accurately determined, as the region near T_N is not complicated by its presence as is typical for continuous transitions.

Figure 4 shows typical longitudinal scans through several magnetic Bragg reflections at $T=2$ K. The magnetic neutron-scattering cross section is proportional to the component of moment perpendicular to $\mathbf{Q}=\mathbf{k}_i-\mathbf{k}_f$ (Ref. 19) and to the square of the magnetic form factor $f(Q)$ which decreases with increasing $|\mathbf{Q}|$. Figure 4 shows in addition to a decrease with $|\mathbf{Q}|$, an angular dependence favoring reflections that lie close to the $\mathbf{c}^*$ axis. This may be seen by comparing the data at $(0.39,0,\frac{3}{2})$, with $|\mathbf{Q}|=2.41$ Å, and at $(1.39,0,\frac{1}{2})$, with $|\mathbf{Q}|=2.09$ Å. Clearly the scattering at $(1.39,0,\frac{1}{2})$, close to the basal plane, is greatly suppressed. The data shown in Fig. 4 provide strong evidence, therefore, that the magnetic moment direction is aligned within the basal plane.

The integrated intensities have been compared with those calculated for several simple models for the magnetic struc-

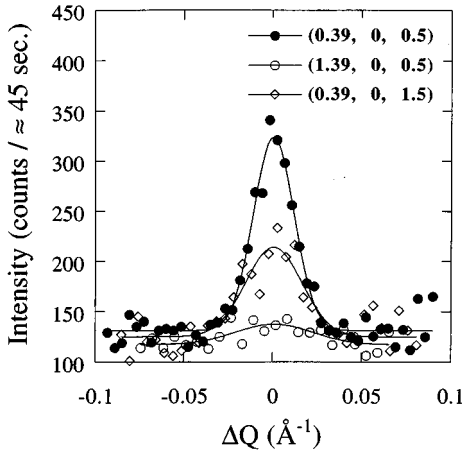

FIG. 4. Typical longitudinal scans at various magnetic ordering wave vectors are shown at 2 K. These are at $\mathbf{Q}=(0.39,0,\frac{1}{2})$, $|\mathbf{Q}|=0.95$ Å^{-1}, $\alpha=34.8°$; $\mathbf{Q}=(0.39,0,\frac{3}{2})$, $|\mathbf{Q}|=2.41$ Å^{-1}, $\alpha=13.0°$; $\mathbf{Q}=(1.39,0,\frac{1}{2})$, $|\mathbf{Q}|=2.09$ Å^{-1}, $\alpha=68.0°$. α refers to the angle between $\mathbf{Q}$ and the $\mathbf{c}^*$ axis.

ture, in which the moments lie within the basal plane, so that

$$I(\mathbf{Q})=\frac{F(\mathbf{Q})^2}{\sin(2\theta)}\sin^2(\nu)f^2(Q), \tag{1}$$

where $F(\mathbf{Q})$ is the structure amplitude for the Bragg peak, and ν is the angle between $\mathbf{Q}$ and the moment direction (in the case of a collinear magnetic structure where a unique moment direction exists; otherwise an appropriate generalization is employed). Both $F(\mathbf{Q})$ and ν depend on the model for the ordered magnetic structure. The magnetic form factor $f(Q)$was that measured[20] for UO_2, which is known to give an adequate account of the properties of several uranium-based magnetic compounds.

The integrated intensities of seven magnetic Bragg positions, corrected for the Lorentz factor $[\sin(2\theta)]^{-1}$ and the magnetic form factor are shown in Fig. 5(a) as a function of α, the angle between $\mathbf{Q}$ and the $\mathbf{c}^*$ direction. As was evident from Fig. 4, the Bragg peak intensities fall off with increasing α. This result eliminates all models in which the magnetic moment is aligned predominantly along $\mathbf{c}^*$, in contrast to a previous suggestion.[16] Two sets of data are shown in Fig. 5(a), both of which come from measurements at CRL. The difference between them is the energies of the neutron beam used, 17.1 meV with no PG filter and 34.1 meV with a PG filter. The relative intensities from these two sets of measurements are consistent, which give confidence that the results are robust to possible systematic errors, such as extinction, or absorption, or higher-order wavelength harmonics. Figure 5(b) shows similar data taken with a vertical magnetic field of 8 T applied to the sample, and will be discussed later.

We examined several simple models of incommensurate magnetic structures in which the magnetic moments lie within the basal plane, as candidates to describe our results. The three which seemed most likely are displayed in Fig. 6. These are the longitudinal spin-density wave (SDW) model with moments polarized along the $\mathbf{a}^*$ direction, the ''nearly longitudinal'' SDW model with moments polarized along either of the two $\mathbf{a}$ directions which lie at $\pm 30°$ to the $\mathbf{a}^*$

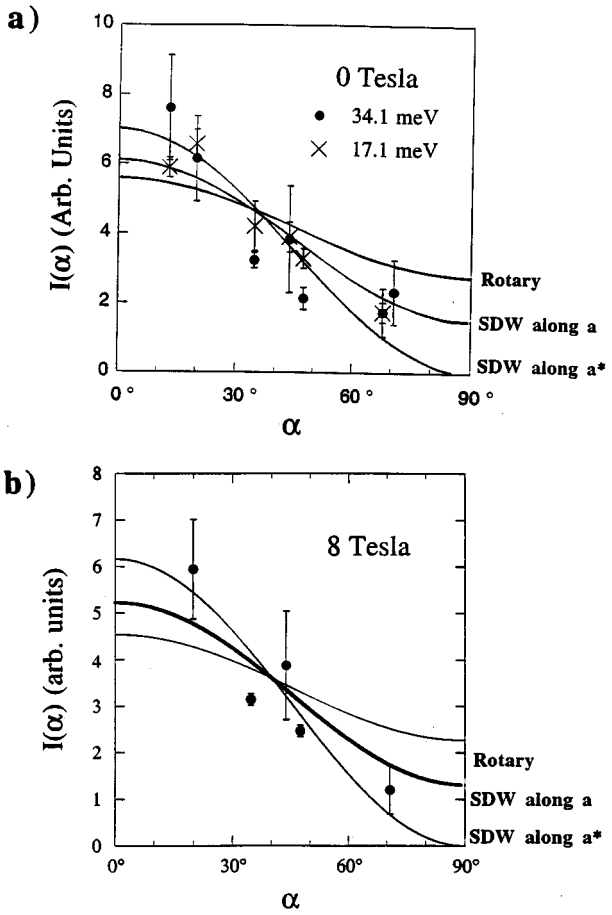

FIG. 5. The intensities of several [seven in (a) and five in (b)] magnetic Bragg reflections, corrected for Lorentz and form factors, are shown as a function of α, the angle between $\mathbf{Q}$ and the $\mathbf{c}^*$ axis. Panel (a) shows these data in the absence of an applied magnetic field, while panel (b) shows data taken in an 8 T vertical magnetic field. All data shown were taken at 2 K. In zero magnetic field [panel (a)] two sets of measurements corresponding to different neutron energies are shown. Their consistency provides confidence that these results are free from systematic errors. The solid lines are comparisons to the expectations of three relatively simple models (see text and Fig. 6) for single-q,incommensurate magnetic structures with the moments constrained to lie within the basal plane. The α dependence is very similar in panels (a) and (b) indicating that no significant change in the magnetic structure occurs on application of the vertical magnetic field.

modulation direction, and the noncollinear rotary model, in which the direction of the magnetic moment is rotated within the basal plane. In all of these models, the spin arrangement shown in Fig. 6 represents a single domain structure within one basal plane. The calculated intensities assume the crystal is composed of three equally populated, equivalent q domains, and an additional two spin domains for the second model. The full three-dimensional structure is made up of a simple antiferromagnetic stacking of the basal plane structures along $\mathbf{c}^*$, corresponding to $Q_c=\frac{1}{2}$.

The α dependence expected from these three models is shown in Figs. 5(a) and 5(b) by three solid lines, one for each of the $\mathbf{a}^*$ SDW model, the $\mathbf{a}$ SDW model, and the rotary model. As can be seen, the rotary structure, in which the *direction* of the moments is modulated within the basal

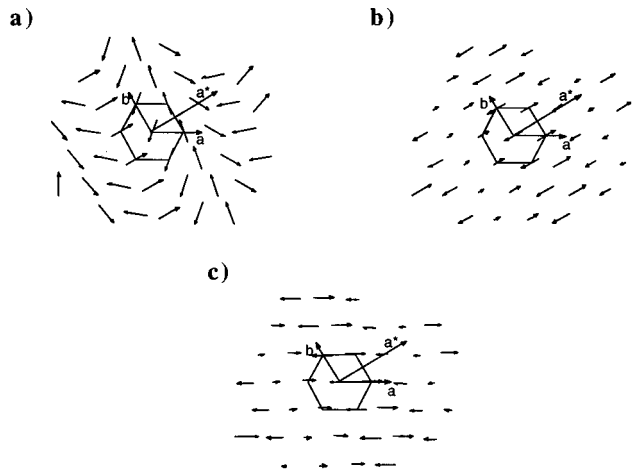

FIG. 6. Real space spin configurations corresponding to a single domain of the incommensurate magnetic structures which were compared with measurements of the magnetic Bragg peak intensities in Fig. 5 are shown. These are (a) the rotary model in which all spins have the same magnitude and the spin direction is modulated along **a***, (b) the collinear, longitudinal spin-density wave (SDW) model in which the moment points either parallel or antiparallel to **a*** and the magnitude of the moment is modulated along **a***, (c) the collinear **a** SDW model in which the moments point either parallel or antiparallel to **a** and the magnitude of the moment is modulated along **a***.

plane, has a less-pronounced α dependence than that of either SDW model, in which the moments are always aligned along either the **a*** or **a** directions, but their *magnitudes* are modulated from site to site. Models in which the moments are aligned along different directions within the basal plane which are progressively more transverse to the **a*** modulation direction, but whose magnitudes are modulated along **a***, so as to give rise to the correct incommensurate component of the ordering wave vector, produce weaker α dependencies than the longitudinal **a*** SDW or the ''nearly longitudinal'' **a** SDW models, with a transverse **a** SDW model exhibiting no α dependence at all. This is due to the sensitivity of the magnetic neutron-scattering cross section to those components of the moment which lie in a plane perpendicular to **Q**.[19] Thus we can exclude a purely transverse SDW in which the polarization is perpendicular to **a***.

A key to understanding all of these dependencies is that measurements at a single ordering wave vector probe only one domain when the structure is single q. If all possible q domains are equally populated, it is not possible from data in zero field and stress to distinguish between a single-q structure and a multiple-q modulated spin structure, such as is known to describe the magnetically ordered state of neodymium.[21] Information about such structures may be obtained indirectly if magnetoelastic effects are present which couple the spins to the lattice. Landau theory for UNi_2Al_3 (Ref. 22) shows that single and triple-q magnetic structures would be accompanied by supplementary nuclear scattering at $(1\text{-}2\tau,0,0)$, while triple-q magnetic structures alone have $(\frac{1}{2}\text{-}\tau,0,0)$ Bragg peaks associated with them. Scans of the form $(h,0,1)$ were carried out to search for such reflections and none was observed, however, we cannot completely rule out a multiple-q structure as the effects may be small.

With the caveat that multiple-q structures may occur, we observe that all of our data are well described (Fig. 5) by either the longitudinal **a*** SDW model or the ''nearly longitudinal'' **a** SDW model. As will be discussed in the next section, the behavior we observe in the presence of a strong magnetic field can be used to distinguish between these two possibilities.

We can estimate the size of the ordered magnetic moment by comparing the magnetic Bragg peak intensities to those of weak nuclear Bragg peaks. Weak nuclear Bragg peaks are employed in this comparison, as they are less likely to be affected by extinction; however, as the role of extinction is not completely understood in these measurements, the estimated moment size represents an upper limit. The size of the ordered moment determined from our data depends weakly on the model under consideration. The **a*** SDW model gives an ordered moment of $0.24\mu_B$, if all three domains of such a single-q structure are equally populated. The corresponding estimate for the **a** SDW model is $0.21\mu_B$. In both cases the magnitude of the ordered moment is modulated from site to site and the rms average ordered moment is $1/\sqrt{2}$ the maximum value.

It is worthwhile commenting on the stability of such modulated spin structures at low temperatures. In other systems where this behavior is observed, e.g., in the longitudinal SDW phase of Er,[23] the structure eventually ''squares up,'' meaning that the moment size becomes equal at all sites, as the temperature is reduced, giving rise to harmonics (at 3τ and 5τ, for example) which are weaker than the fundamental. Behavior of this sort was searched for but was not observed, indicating either that the modulated spin structure is stable to the lowest temperatures, or that the harmonics are too weak to observe.

MEASUREMENTS IN A MAGNETIC FIELD

Measurements were also made in a magnet cryostat which allowed the application of a vertical magnetic field up to 8 T. The measurements, performed on the N5 triple axis spectrometer at CRL, were carried out in elastic-scattering geometry with Si(1,1,1) as monochromator, PG(0,0,2) as analyzer, a neutron energy of 14.5 meV, and a PG filter placed in the scattered beam to remove higher order contamination. The collimation was 0.55° on the incident side and 0.60° on the scattered side. The lowest temperature which could be accessed was 2 K, above the superconducting $T_C \sim 1.2$ K, but sufficiently far below T_N to study the field dependence of the low-temperature magnetic structure.

Scans of the form $(h,0,\frac{1}{2})$ taken at 2 K as a function of vertical field are shown in Fig. 7. As depicted in the lower part of Fig. 7, the field is directed along **b**, equivalent to **a** and a near-neighbor direction within the basal plane. The complicated line shapes displayed in these scans, particularly near $(0.39,0,\frac{1}{2})$ arise from the mosaic of the sample. Two features are clear in these data. First the integrated intensities of the magnetic Bragg peaks increase markedly above fields of $\sim$3 T. Second, the superlattice peak positions move further away from $h=\frac{1}{2}$ along h and therefore from each other,

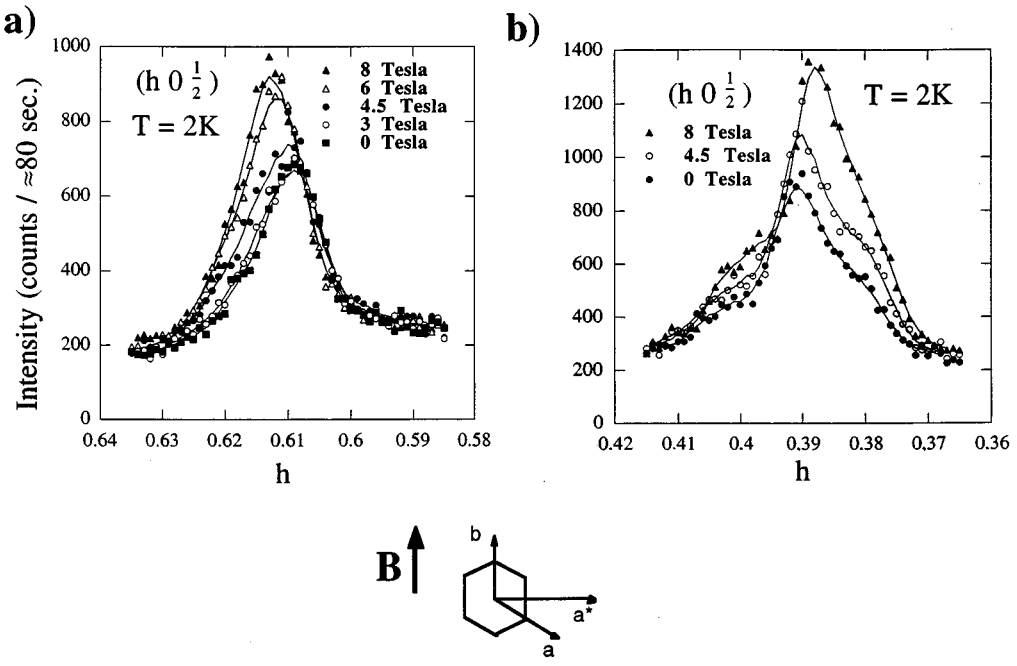

FIG. 7. Elastic neutron scattering scans of the form $(h,0,\frac{1}{2})$ in the presence of various values of the vertical magnetic field strength, at 2 K are shown. The asymmetric line shapes are due to the sample mosaic. The diagram at the bottom of the figure shows that the field direction lies in the basal plane along **b**, a near-neighbor direction equivalent to **a**.

as the field strength is increased, indicating that the incommensurate part of the ordering wave vector, τ in $(\frac{1}{2}\pm\tau,0,\frac{1}{2})$, is field dependent at these low temperatures. This behavior is summarized in Fig. 8. It can be seen that both the integrated intensity of the superlattice peaks as well as their reciprocal space position appear to move from one relatively stable value to another over the field range 4 to 6 T. The integrated intensity increases by a factor of 1.55 ± 0.07. Also, there is little or no hysteresis: decreasing the magnitude of the applied field brings the magnetic superlattice peaks back to their original positions and intensities.

Despite the strong field dependencies mentioned above, there is little or no field dependence to either T_N or the magnetic structure which the material enters below T_N. In Fig. 9 we show that the onset of long-range magnetic order in vertical fields up to 8 T occurs with no measurable shift in T_N. Figure 5(b) shows the α dependence of the corrected intensities of several superlattice Bragg peaks in the presence of an 8 T vertical magnetic field. Once again α is the angle between **Q** and the **c** axis, and the same corrections which were made for the magnetic form factor and Lorentz factor for the data in Fig. 5(a) have again been made. There is no evidence for a change in the magnetic structure as a function of field.

Taken together, these results strongly suggest that the 1.55 times growth with field of the magnetic superlattice Bragg peak intensities is related to changes in the domain population. A ratio of 1.5 is consistent with the number of

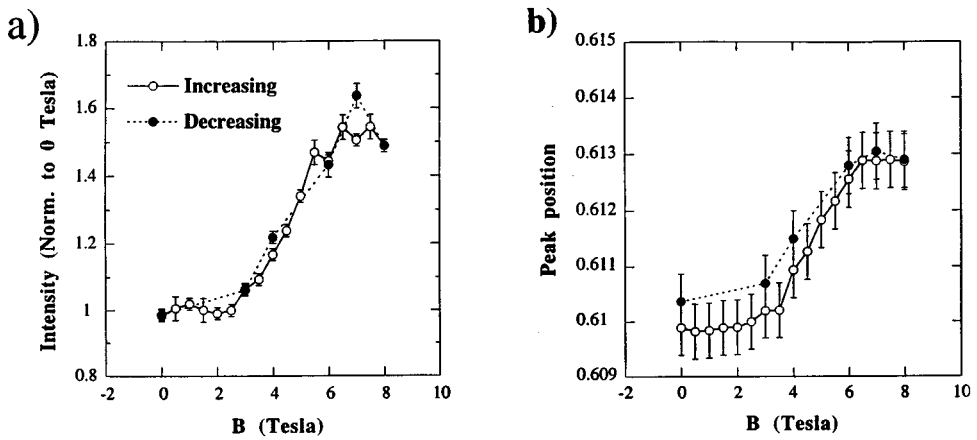

FIG. 8. (a) The integrated intensity of the $(h,0,\frac{1}{2})$ scans of Fig. 7 at 2 K as a function of vertical magnetic field. (b) The peak position, $h=\frac{1}{2}+\tau$, also from fits to the data shown in Fig. 7.

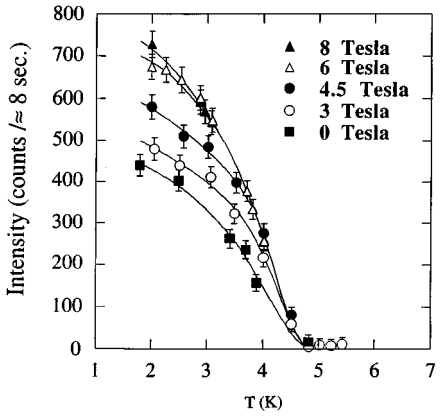

FIG. 9. Order parameters measured at $\mathbf{Q}=(0.61,0,\frac{1}{2})$ as a function of vertical magnetic field strength. It is clear that there is little or no field dependence to T_N.

occupied domains being reduced by the field to $\frac{2}{3}$ of its zero field value, so that the volume fraction of the crystal contributing to any one superlattice reflection changes from $\frac{1}{3}$ to $\frac{1}{2}$. Using a sketch of domain selection by magnetic field in Fig. 10 we can show that these results favor the **a** SDW model for which the field reduces the number of domains from 6 to 4. The longitudinal SDW of the **a*** SDW model can be eliminated because the field selects a single domain and should have caused a threefold growth in Bragg intensity with field. However, for the **a** polarized SDW model there are six domains arising from two spin domains for each of the three equivalent wave vector domains. Only two of the six domains are unfavorable in the field and all of the others are equally favorable. Therefore we expect the field to decrease the number of **a** SDW domains from 6 to 4, resulting in the observed 50% increase in intensity. We conclude that our full data set is described by an **a** polarized SDW structure. It should be noted that all of the above arguments depend on the assumption that the intensity and peak position changes have saturated by 8 T, as suggested by Fig. 8.

An interesting feature of these field effects is that they display no hysteresis. This is not expected of strictly domain population effects; while symmetry dictates that equal populations of the equivalent domains will form in the absence of a symmetry-breaking field, once the domain population has been unbalanced, the new population is expected to be stable even if the symmetry-breaking field is then reduced in intensity to zero. The lack of hysteresis may be due to the change in incommensurate ordering wave vector induced by the field. The associated strain changes may provide the energy to re-equilibrate the domain populations.

The temperature dependence of the incommensurate part τ of the ordering wave vector also displays interesting behavior as shown in Fig. 11. There is no temperature dependence to τ in the absence of a magnetic field, but in the presence of an 8 T vertical field, τ relaxes to its zero field value on heating. This behavior is summarized in panel (c) of Fig. 11. This is of interest for several reasons. First, it is clear from panel (c) that τ is field independent near T_N, and only takes on a field dependence at low temperatures. Second, the temperature dependence of an incommensurate wave vector is often taken as a signature of *itinerant* spin-density wave

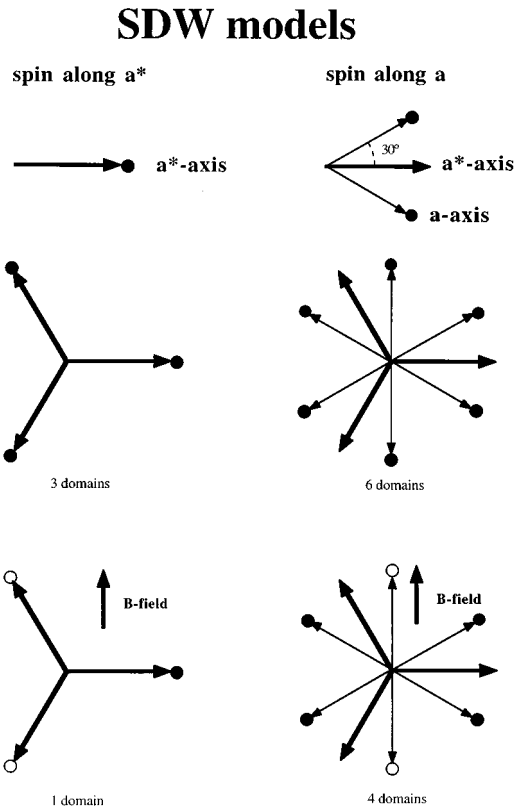

FIG. 10. The domains associated with each of the **a*** and **a** SDW models are shown. The three **a*** modulation directions are shown as thick arrows. The two spin polarizations for each wave vector domain of the **a**-polarized SDW are shown by thin arrows. The domains which survive the application of a vertical magnetic field are indicated with filled circles while those which do not are indicated with open circles. Accordingly, one of three **a*** SDW domains survives the application of a (sufficiently strong) vertical field, resulting in an expected threefold increase in the Bragg intensity for this model. Four of six survive in the **a** SDW case, resulting in an anticipated increase of a factor of 1.5 in the Bragg intensity, as is observed [see Fig. 8(a)].

behavior. A continuous evolution with temperature of the incommensurate wave vector is observed, for example, in the $3d$ SDW magnet chromium,[24] but not in the localized $4f$ SDW magnet erbium.[23] Our results suggest that the magnetism in UNi_2Al_3 becomes itinerant, or more itinerant, in the presence of vertical magnetic fields in excess of $\sim$4 T.

A further interesting effect in the presence of a vertical magnetic field was observed in the behavior of the *nuclear* Bragg peaks. This is demonstrated in Fig. 12, panel (a) of which shows a radial scan of the (1,0,2) nuclear Bragg position at 2 K in zero magnetic field and also in a vertical applied magnetic field of 8 T. There is clearly more intensity present in the presence of the magnetic field. Panel (b) of Fig. 12 shows the relative change of five nuclear Bragg peaks as the field is increased at 2 K, while panel (c) shows the difference between the 8 T integrated intensity and the zero field integrated intensity for the same five nuclear Bragg peaks at 2 T. Two features are evident. First the excess intensity grows linearly with increasing field strength, and second the dependence of this excess intensity on $|\mathbf{Q}|$ is very unusual. This effect is *not* related to the long-range magnetic

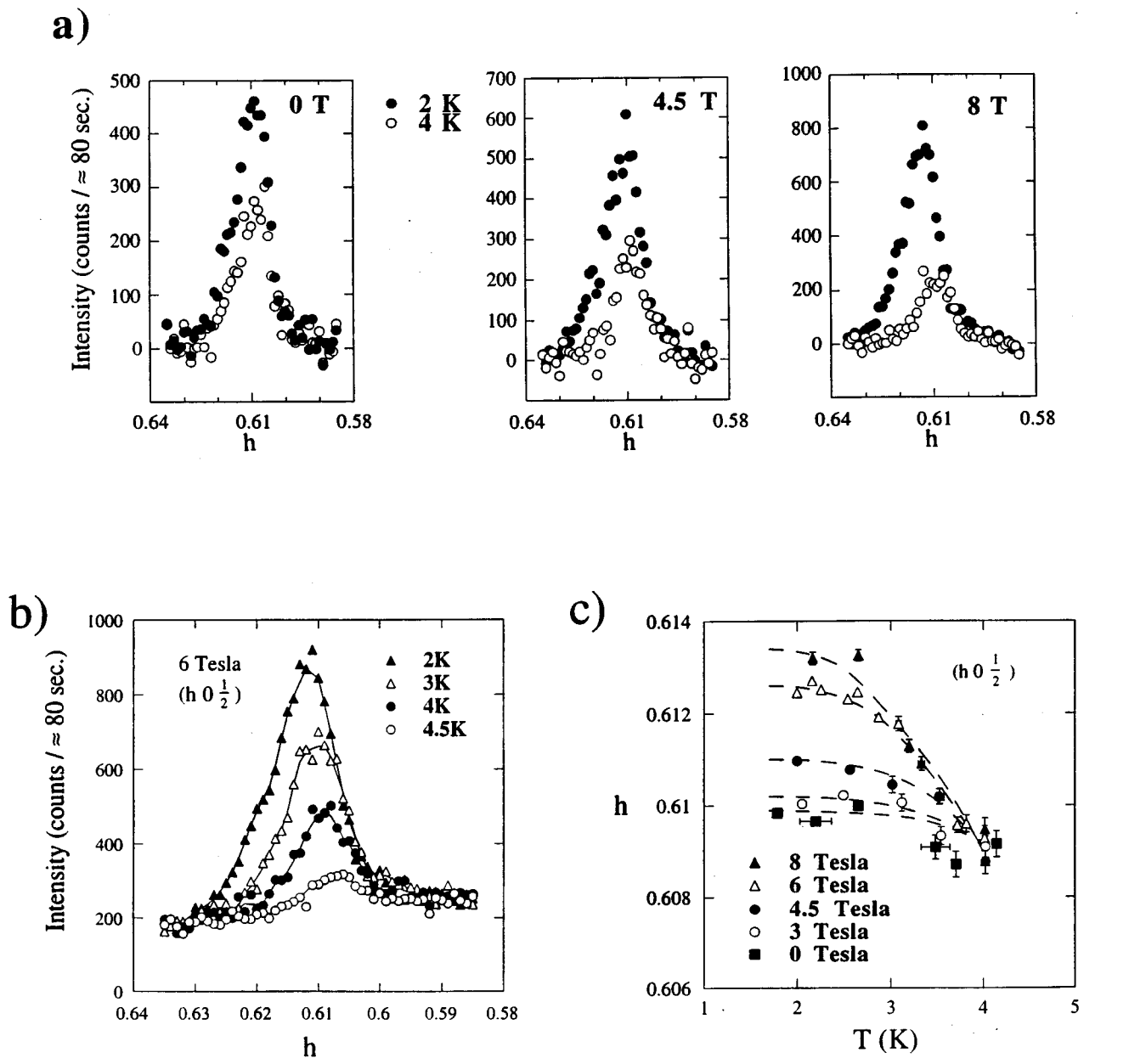

FIG. 11. (a) Elastic scattering scans of the form $(h,0,\frac{1}{2})$ near $h=0.61$ for various values of the vertical magnetic field for 2 and 4 K. (b) Scans of the form $(h,0,\frac{1}{2})$ near $h=0.61$ at various temperatures below T_N for a vertical field of 6 K. (c) The results for the field and temperature dependence of the incommensurate part, $h=\frac{1}{2}+\tau\sim 0.61$, of the magnetic ordering wave vector. This plot summarizes the data in (a) and (b). It demonstrates that τ is temperature independent in zero field, but acquires significant temperature dependence for vertical applied magnetic fields in excess of ~4 T.

order in the system, as this field dependence has been observed at temperatures as high as 25 K. It may be that it correlates with the coherence temperature ~80 K as indicated by the ''hump'' in the uniform susceptibility,[11] but measurements to date have not been made above 25 K.

One might expect there to be some magnetic contribution to the nuclear Bragg peaks induced by the presence of a strong field. Were this the cause of the extra scattering the **Q** dependence of the scattering would simply reflect the magnetic form factor of the system, which decreases monotonically with $|\mathbf{Q}|$. This is clearly not the case, as is illustrated in panel (c) of Fig. 12. The $|\mathbf{Q}|$ dependence is remarkably well described by a simple parabola, with large effects at both large and small values of $|\mathbf{Q}|$. This effect can also not be explained by the induced moments canting along another direction not parallel to the field, as the change between (1,0,1) and (2,0,2) as well as the change between (1,0,0) and (2,0,0), which are two pairs of parallel wave vectors, go in opposite direction to each other. Such an effect therefore cannot be due to the sensitivity of the magnetic neutron-scattering cross section to components of moment which lie in a plane perpendicular to **Q**.[19] While we do not understand this behavior, we believe that it cannot be explained on the basis of magnetic scattering alone, and may arise from a

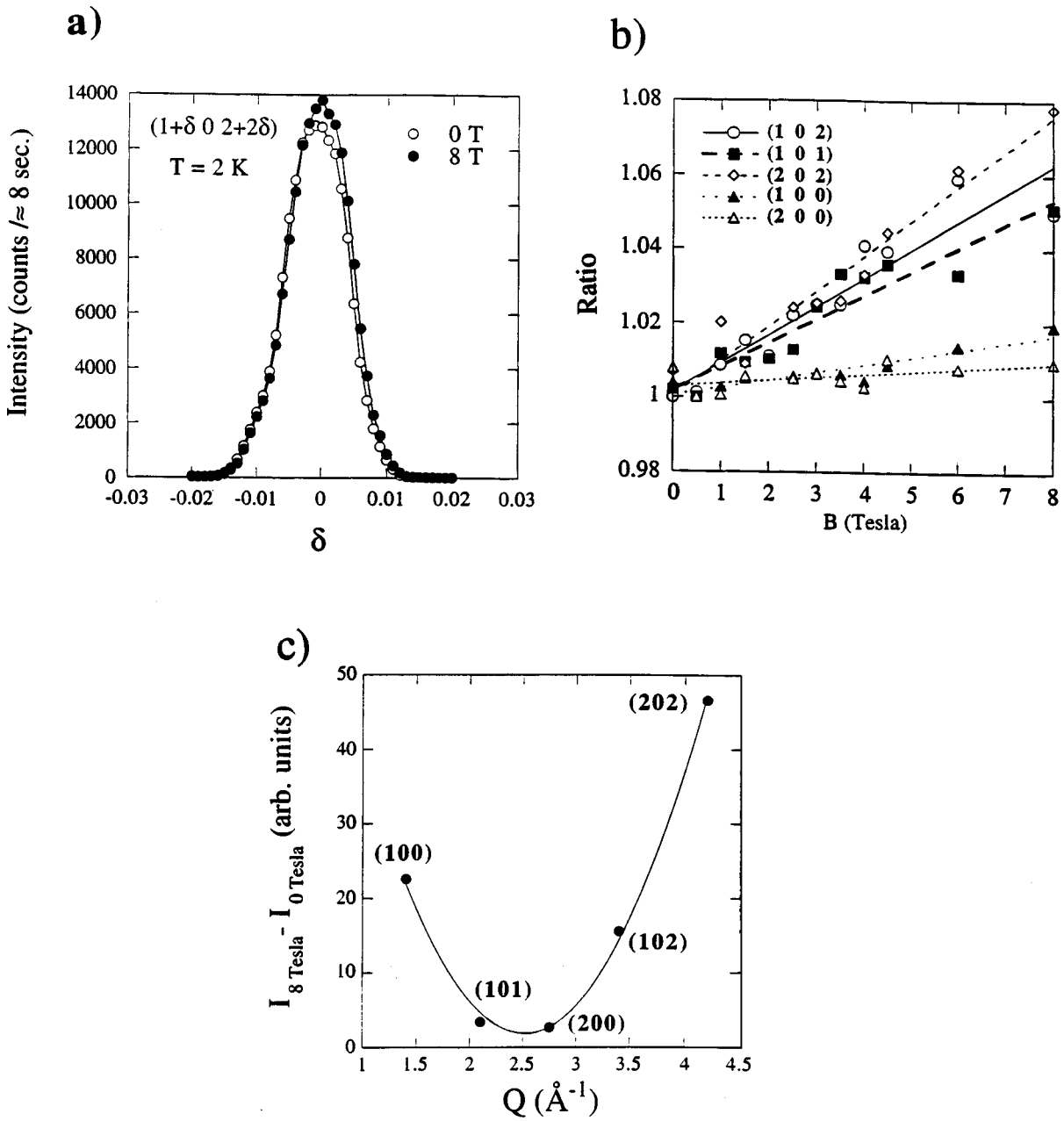

FIG. 12. (a) Longitudinal elastic scattering of the (1,0,2) nuclear Bragg position at 2 K in zero magnetic field and in a vertical magnetic field of 8 T. Excess scattering in the presence of the 8 T field is evident. (b) The field dependence of the relative (to zero field) strength of five different nuclear Bragg peaks. (c) The difference between the nuclear Bragg peak intensities for five nuclear reflections in zero field and in an 8 T vertical magnetic field as a function of $|\mathbf{Q}|$. This plot demonstrates that the field dependence of the intensity at the nuclear positions cannot be understood by any simple model involving the magnetism alone. The data in (b) and (c) originate from longitudinal scans of the appropriate nuclear Bragg peaks, e.g., (1,0,2) shown in (a).

coupling between the magnetism (although not the long-range ordered component) and the lattice.

LOW-TEMPERATURE MEASUREMENTS WITHIN THE SUPERCONDUCTING PHASE

Elastic-scattering measurements were performed on the H8 triple axis spectrometer at BNL using a ^{3}He refrigerator equipped with a 6.5 T vertical magnetic field. This allowed us access to temperatures well below $T_C \sim 1.2$ K, and to magnetic fields considerably larger than the upper critical field $H_{C2} \sim 1.4$ T, as measured on polycrystalline materials.[25] The measurements were performed with PG(0,0,2) as both monochromator and analyzer and 14.5 meV neutrons. Graphite filters were placed in both the incident and scattered beams to reduced higher order contamination, and the collimation was 40′-20′-20′-80′.

Figure 13 shows the order parameter as measured at $(0.39,0,\frac{1}{2})$ down to $\sim$0.45 K, both in zero field and in an applied vertical field of 5 T. The elastic scattering is about 30% stronger in the presence of the 5 T field, consistent with our earlier measurements. A comparison between the *form* of

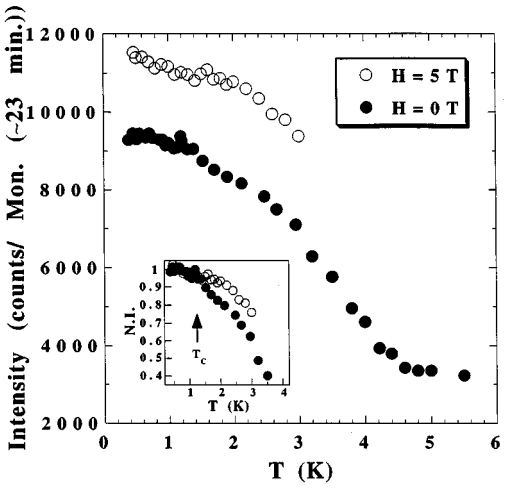

FIG. 13. The magnetic order parameter as measured at the $(0.39,0,\frac{1}{2})$ position, for temperatures as low as 0.45 K, well below the superconducting $T_C \sim 1.2$ K. The inset displays differences in the form of the order parameter (see text) between that measured in zero field and that measured in a 5 T vertical field, greater than H_{C2}, which can be seen above $T_C \sim 1.2$ K. This indicates a substantial coupling between the antiferromagnetic and superconducting order parameters.

the order parameters at low temperatures is shown in inset of Fig. 13 and is intriguing. This plot (labeled N.I. for normalized intensity) shows the elastic scattering, with background subtracted, normalized to agree at the lowest temperatures. A break in the temperature dependence between the superconducting sample in zero field and the nonsuperconducting sample, in a vertical field of 5 T, occurs near $T_C \sim 1.2$ K.

A comparison between the field dependence of the antiferromagnetic Bragg intensity below and above the superconducting transition is shown in Fig. 14. Here we show the magnetic Bragg intensity, again at $(0.39,0,\frac{1}{2})$, for temperatures of 1.6 K [above $T_C(H=0)$] and 0.45 K [below $T_C(H=0)$]. These scans have an advantage over the data presented in Fig. 13 in that the effect of the magnetic field on the domain population is the same at each temperature, thus normalization is not required in the comparison. This comparison is both qualitatively and quantitatively consistent with that shown in Fig. 13. The antiferromagnetic order parameter is about 3% higher (the elastic scattering is proportional to the square of the order parameter) in the superconducting phase at 0.45 K than in the low temperature, normal phase at 1.6 K, and this difference is maintained until the field strength exceeds a value of ~4 T. Measurements of H_{C2} on single crystals of UNi_2Al_3have not yet been performed. Our results suggest $H_{C2} \sim 4$ T for fields applied along the **a** direction.

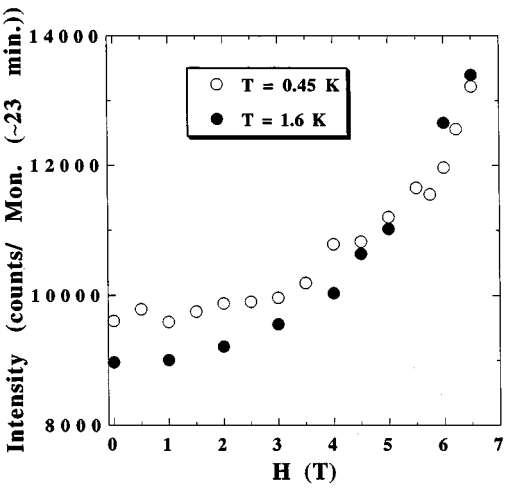

FIG. 14. The vertical field dependence of the magnetic order parameter as measured at $(0.39,0,\frac{1}{2})$ and 0.45 K, well below the superconducting $T_C \sim 1.2$ K as well as at 1.6 K, which is well above T_C. These data, consistent with that shown in Fig. 16, indicate that the antiferromagnetic order parameter is enhanced by as much as 3% on entering the superconducting phase.

These results indicate a strong coupling between the superconducting and antiferromagnetic order parameters. Such coupling has also been observed in UPt_3,[26,27] but with the opposite effect; the antiferromagnetic order parameter is *depressed* on entering the superconducting phase. Similar behavior has not been observed in either URu_2Si_2 (Ref. 28) or in UPd_2Al_3.[13,14]

That the behavior we observe in UNi_2Al_3 bears similarities to that observed in UPt_3 does not surprise us. In both materials, the moments lie within the basal plane, and the antiferromagnetic structure along **c** is a simple stacking of the basal plane magnetic structure. Further, studies of the inelastic scattering from UNi_2Al_3 (Ref. 29) show the spectrum of dynamic spin fluctuations also has similarities with that in UPt_3.

Finally, it is worthwhile noting that to within our resolution, the magnetic Bragg peaks are resolution limited at all temperatures measured. We therefore conclude that the coexistence between the superconductivity and antiferromagnetism in UNi_2Al_3 is microscopic.

CONCLUSIONS

Elastic neutron-scattering measurements have been carried out at temperatures near to and below $T_N \sim 4.6$ K in UNi_2Al_3. These measurements were made both in the absence and presence of a magnetic field directed vertically, and hence along an **a** direction for scans of the form $(h,0,1)$, and also at temperatures well below the superconducting $T_C \sim 1.2$ K.

These measurements have produced three principal results: a detailed magnetic structure including domain selection by a vertical magnetic field; precise information on the critical phenomena associated with the magnetic transition; and direct evidence for coupling between the superconducting and antiferromagnetic order parameters at low temperature.

Specifically, we observe the appearance of superlattice magnetic Bragg peaks characterized by ordering wave vectors of the form $(\frac{1}{2}\pm\tau,0,\frac{1}{2})$, with $\tau=0.110\pm0.003$, indicating an incommensurate magnetic structure within the basal plane, which is simply stacked antiferromagnetically along **c** to form the full three-dimensional magnetic structure. The relative intensities of the magnetic Bragg peaks can be described by a spin-density wave structure within the basal plane, where the moment direction is within the basal plane,

but the magnitude of the ordered moment is modulated from site to site along **a***. It is clear that most of the ordered moment lies within the basal plane. By application of a vertical magnetic field to select domains, we find the spin direction lies along **a** at 30° to the **a*** modulation direction. We also find a shift in τ, the incommensurate part of the ordering wave vector, with increasing field, suggesting itinerant behavior. The maximum amplitude of the ordered moment is estimated to be $0.21\mu_B \pm 0.10$, which, while small compared to the magnitude of ordered moments in most magnets, is comparable to those observed in other heavy-fermion superconductors.

The long-range order magnetic structure of UNi_2Al_3 bears little resemblance to that of its sister hexagonal heavy-fermion superconductor UPd_2Al_3, which exhibits a simple antiferromagnetic stacking of ferromagnetic basal plane sheets and a large ordered moment of $\sim 0.85\mu_B$.[12,13] However, the form of the magnetic order parameter, at least at temperatures above $T_N/2$, is similar in the two materials, with approximately conventional three-dimensional critical behavior displayed in each, in contrast to the anomalous linear behavior of the superlattice intensity with temperature displayed by both UPt_3 (Ref. 2) and URu_2Si_2.[6,7] We find that the antiferromagnetic order parameter is enhanced by about 3% on entering the superconducting state, which demonstrates strong coupling between the superconducting and antiferromagnetic order parameters.

ACKNOWLEDGMENTS

This work has benefitted from conversations with B. Sternlieb, G. Luke, Y. J. Uemura, E. Lorenzo-Diaz, and R. S. Fishman. We are grateful to J. S. Gardner for help in producing the figures. Four of us (J.G.L., M.M., A.S., and B.D.G.) gratefully acknowledge the hospitality of both the Chalk River Laboratories and Brookhaven National Laboratory. This work was supported in part by the Natural Sciences and Engineering Research Council of Canada, the Ontario Centre for Materials Research, and FCAR du Quebec. Work at Brookhaven National Laboratory was supported by the DMS of the U.S. DOE under Contract No. DEACO276CH00016. One of us (B.D.G.) acknowledges the support of the Alfred P. Sloan Foundation.

*Present address: Lawrence Livermore National Laboratory, P.O. Box 808, M/S L-395, Livermore, CA 94550.

†Present address: Physikalisches Institut, Universitaet Karlsruhe D-786128, Karlsruhe, Germany.

[1] Recent reviews of this topic can be found in N. Grewe and F. Steglich, *Handbook on the Physics and Chemistry of Rare Earths*, edited by K. A. Gschneider, Jr. and L. Eyring (Elsevier, New York, 1991), Vol. 14, Chap. 97, p. 343; A. de Visser and J. J. M. Franse, J. Magn. Magn. Mater. **100**, 204 (1991); G. Aeppli and C. Broholm, *Handbook on the Physics and Chemistry of Rare Earths*, edited by K. A. Gschneider, Jr. and L. Eyring (Elsevier, New York, 1994), Vol. 19, Chap. 131, p. 123; R. H. Heffner and M. R. Norman, Comments Condens. Matter Phys. **17**, 361 (1996).

[2] G. Aeppli, E. Bucher, C. Broholm, J. K. Kjems, J. Baumann, and J. Hufnagl, Phys. Rev. Lett. **60**, 615 (1985).

[3] K. Hasselbach, L. Taillefer, and J. Flouquet, Phys. Rev. Lett. **63**, 93 (1989).

[4] S. M. Hayden, L. Taillefer, C. Vettier, and J. Flouquet, Phys. Rev. B **46**, 8675 (1992); M. Boukhny, G. L. Bullock, B. S. Shivaram, and D. G. Hinks, Phys. Rev. Lett. **73**, 1707 (1994).

[5] T. T. M. Palstra, A. A. Menovsky, J. van der Berg, A. J. Dirkmaat, P. H. Kes, G. J. Nieuwenhuys, and J. A. Mydosh, Phys. Rev. Lett. **55**, 2727 (1985).

[6] C. Broholm, J. K. Kjems, W. J. L. Buyers, P. Matthews, T. T. M. Palstra, A. A. Menovsky, and J. A. Mydosh, Phys. Rev. Lett. **58**, 1467 (1987); C. Broholm, H. Lin, P. T. Matthews, T. E. Mason, W. J. L. Buyers, M. F. Collins, A. A. Menovsky, J. A. Mydosh, and J. K. Kjems, Phys. Rev. B **43**, 12 809 (1991).

[7] E. D. Isaacs, D. B. McWhan, R. N. Kleiman, D. J. Bishop, G. E. Ice, P. Zschack, B. D. Gaulin, T. E. Mason, J. D. Garrett, and W. J. L. Buyers, Phys. Rev. Lett. **65**, 3185 (1990); T. E. Mason, B. D. Gaulin, J. D. Garrett, Z. Tun, W. J. L. Buyers, and E. D. Isaacs, *ibid.* **65**, 3189 (1990).

[8] V. Barzykin and L. P. Gor'kov, Phys. Rev. Lett. **70**, 2479 (1993).

[9] M. B. Walker, W. J. L. Buyers, Z. Tun, W. Que, A. A. Menovsky, and J. D. Garrett, Phys. Rev. Lett. **71**, 2630 (1993); W. J. L. Buyers, Physica B **223-224**, 9 (1994).

[10] C. Geibel, C. Schank, S. Thies, H. Kitazawa, C. D. Bredl, A. Böhm, M. Rau, A. Grauel, R. Casparay, R. Helfrich, U. Ahlheim, G. Weber, and F. Steglich, Z. Phys. B **84**, 1 (1991).

[11] C. Geibel, S. Thies, D. Kaczororowski, A. Mehner, A. Grauel, B. Seidel, U. Ahlheim, R. Helfrich, K. Petersen, C. D. Bredl, and F. Steglich, Z. Phys. B **83**, 305 (1991).

[12] A. Krimmel, P. Fischer, B. Roessli, H. Maletta, C. Geibel, C. Schank, A. Grauel, A. Loidl, and F. Stegich, Z. Phys. B **86**, 161 (1992).

[13] T. Petersen, T. E. Mason, G. Aeppli, A. P. Ramirez, E. Bucher, and R. N. Kleiman, Physica B **199-200**, 151 (1994); T. E. Mason, T. Petersen, G. Aeppli, W. J. L. Buyers, E. Bucher, J. D. Garrett, K. N. Clausen, and A. A. Menovsky, *ibid.* **213-214**, 11 (1995).

[14] B. D. Gaulin, D. Gibbs, E. D. Isaacs, J. G. Lussier, J. N. Reimers, A. Schröder, L. Taillefer, and P. Zschack, Phys. Rev. Lett. **73**, 890 (1994).

[15] A. Schröder, J. G. Lussier, B. D. Gaulin, J. D. Garrett, W. J. L. Buyers, L. Rebelsky, and S. M. Shapiro, Phys. Rev. Lett. **72**, 136 (1994); J. G. Lussier, A. Schröder, B. D. Gaulin, J. D. Garrett, W. J. L. Buyers, L. Rebelsky, and S. M. Shapiro, Physica B **199-200**, 137 (1994).

[16] A. Amato, C. Geibel, F. N. Gygax, R. H. Heffner, E. Knetsch, D. E. MacLaughlin, C. Schank, A. Schenk, F. Steglich, and M. Weber, Z. Phys. B **86**, 159 (1992).

[17] Y. J. Uemeura and G. M. Luke, Physica B **186-188**, 223 (1993).

[18] M. F. Collins, *Magnetic Critical Scattering* (Oxford University Press, New York, 1989).

[19] S. W. Lovesey, *Theory of Neutron Scattering from Condensed Matter* (Clarendon Press, Oxford, 1984), Vol. 2.

[20] G. H. Lander, J. Faber, Jr., A. J. Freeman, and J. P. Desclaux, Phys. Rev. B **13**, 1177 (1976).

[21] E. M. Forgan, J. Magn. Magn. Mater. **104-107**, 1485 (1992); P. Bak and B. Lebech, Phys. Rev. Lett. **40**, 800 (1978).

[22] M. B. Walker (private communication).

[23] H. Lin, M. F. Collins, T. M. Holden, and W. Wei, J. Magn. Magn.

Mater. **104-107**, 1511 (1992), and references therein.
[24] E. Fawcett, Rev. Mod. Phys. **60**, 209 (1988).
[25] F. Steglich *et al.*, Z. Phys. C **195**, 379 (1991).
[26] G. Aeppli, D. Bishop, C. Broholm, E. Bucher, K. Siemensmeyer, M. Steiner, and N. Stüsser, Phys. Rev. Lett. **63**, 676 (1989).
[27] E. D. Isaacs, P. Zschack, C. L. Broholm, C. Burns, G. Aeppli, A. P. Ramirez, T. T. M. Palstra, R. W. Erwin, N. Stücheli, and E. Bucher, Phys. Rev. Lett. **75**, 1178 (1995).
[28] W. Wei, Z. Tun, W. J. L. Buyers, B. D. Gaulin, T. E. Mason, J. D. Garrett, and E. D. Isaacs, J. Magn. Magn. Mater. **108**, 77 (1992).
[29] B. D. Gaulin, M. Mao, S. M. Shapiro, and J. D. Garrett (unpublished).